

Video Article

# Combined Invasive Subcortical and Non-invasive Surface Neurophysiological Recordings for the Assessment of Cognitive and Emotional Functions in Humans

Carlos Trenado<sup>1</sup>, Saskia Elben<sup>2</sup>, David Petri<sup>2</sup>, Jan Hirschmann<sup>2</sup>, Stefan J. Groiss<sup>1,2</sup>, Jan Vesper<sup>3</sup>, Alfons Schnitzler<sup>1,2</sup>, Lars Wojtecki<sup>1,2</sup>

<sup>1</sup>Institute of Clinical Neuroscience and Medical Psychology, Medical Faculty, Heinrich-Heine-University

<sup>2</sup>Department of Neurology, Center for Movement Disorders and Neuromodulation, University Clinic Düsseldorf

<sup>3</sup>Department of Neurosurgery, Functional Neurosurgery and Stereotaxy, Center for Movement Disorders and Neuromodulation, University Clinic Düsseldorf

Correspondence to: Lars Wojtecki at [lars.wojtecki@med.uni-duesseldorf.de](mailto:lars.wojtecki@med.uni-duesseldorf.de)

URL: <https://www.jove.com/video/53466>

DOI: [doi:10.3791/53466](https://doi.org/10.3791/53466)

**Keywords:** Behavior, Issue 111, Invasive subcortical recording, non-invasive neurophysiological recording, cognitive function, emotional function, deep brain stimulation, electroencephalography, neuropsychiatry, brain disorders, clinical neuroscience, neural oscillatory activity, local field potential, electroencephalogram

Date Published: 5/19/2016

**Citation:** Trenado, C., Elben, S., Petri, D., Hirschmann, J., Groiss, S.J., Vesper, J., Schnitzler, A., Wojtecki, L. Combined Invasive Subcortical and Non-invasive Surface Neurophysiological Recordings for the Assessment of Cognitive and Emotional Functions in Humans. *J. Vis. Exp.* (111), e53466, doi:10.3791/53466 (2016).

## Abstract

In spite of the success in applying non-invasive electroencephalography (EEG), magneto-encephalography (MEG) and functional magnetic resonance imaging (fMRI) for extracting crucial information about the mechanism of the human brain, such methods remain insufficient to provide information about physiological processes reflecting cognitive and emotional functions at the subcortical level. In this respect, modern invasive clinical approaches in humans, such as deep brain stimulation (DBS), offer a tremendous possibility to record subcortical brain activity, namely local field potentials (LFPs) representing coherent activity of neural assemblies from localized basal ganglia or thalamic regions. Notwithstanding the fact that invasive approaches in humans are applied only after medical indication and thus recorded data correspond to altered brain circuits, valuable insight can be gained regarding the presence of intact brain functions in relation to brain oscillatory activity and the pathophysiology of disorders in response to experimental cognitive paradigms. In this direction, a growing number of DBS studies in patients with Parkinson's disease (PD) target not only motor functions but also higher level processes such as emotions, decision-making, attention, memory and sensory perception. Recent clinical trials also emphasize the role of DBS as an alternative treatment in neuropsychiatric disorders ranging from obsessive compulsive disorder (OCD) to chronic disorders of consciousness (DOC). Consequently, we focus on the use of combined invasive (LFP) and non-invasive (EEG) human brain recordings in assessing the role of cortical-subcortical structures in cognitive and emotional processing through experimental paradigms (e.g. speech stimuli with emotional connotation or paradigms of cognitive control such as the Flanker task), for patients undergoing DBS treatment.

## Video Link

The video component of this article can be found at <https://www.jove.com/video/53466/>

## Introduction

Invasive neurophysiological recordings in humans date back to seminal studies targeting electrocorticographic recordings from cortical areas and the cerebellum during epilepsy surgery and tumor research<sup>1</sup>. A critical milestone into further development of such recording procedure has been the introduction of the stereotactic technique that provides safe and efficient access to deep structures of the human brain<sup>2</sup>. Apart from clinical treatment, brain invasive approaches in humans provide a rather unique opportunity to study brain function in relation to recorded activity patterns modulated by external stimuli, notably the case of intra- and post-operative invasive recordings in patients undergoing deep brain stimulation (DBS) procedures. The applicability and usefulness of DBS has been addressed in various neurological and neuropsychiatric diseases from Parkinson's disease (PD) to obsessive compulsive disorder (OCD) or conditions like chronic disorders of consciousness (DOC).

In particular, DBS has been applied in the treatment of Parkinson's disease<sup>3,4,5</sup>, essential tremor<sup>6</sup>, primary/generalized segmental dystonia<sup>7,8,9</sup>, Huntington's disease<sup>10,11</sup>, treatment-resistant depression<sup>12,13</sup>, nicotine and alcohol addiction<sup>14</sup>, Alzheimer's disease<sup>15,16</sup>, Tourette's syndrome<sup>17</sup> and chronic disorder of consciousness (DOC)<sup>18,19,20</sup>.

Within the scope of neuropsychiatry, DBS is an approved/CE-marked treatment for obsessive compulsive disorder (OCD) targeting the anterior limb of the internal capsule (ALIC) and is in use targeting the ventral capsule/ventral striatum/ventral caudate (VC/VS), nucleus accumbens (Nac) and the subthalamic nucleus (STN)<sup>21</sup>. Regarding DBS in OCD<sup>22</sup>, recent studies emphasize the role of STN into the mechanism of compulsive checking by utilizing memory based-paradigms<sup>23,24,25</sup>.

Noteworthy, modulation of brain activity under the influence of paradigms with cognitive and emotional connotation has been emphasized in DOC<sup>26,27,28,29</sup>. Thus, DBS is highlighted not only as a prospective treatment for chronic DOC, but also as a clinical procedure that opens up the possibility of studying the modulation of subcortical activity by recording local field potentials (LFP) from central thalamic regions intra- and post-operatively.

In DBS, neurosurgical implantation of electrodes is based on the stereotactic technique that safely accounts for brain anatomical constraints, while patient's stimulation is customized through intra-operative impulse-stimulation tests. Post-operative LFP recording is possible after initial implantation of DBS electrodes and before internalization of the impulse generator. In particular, the present protocol is centered on post-operative recordings.

In combination with LFPs, simultaneous recording of cortical brain activity can be achieved for instance by non-invasive electroencephalography (EEG) or magnetoencephalography (MEG)<sup>30,31</sup>. These two non-invasive methods are supported due to its excellent time resolution. While MEG is less affected than EEG by skull effects<sup>32</sup>, EEG appears advantageous because it is less affected by artifacts caused by metallic implants and head movements and it can be used at the patient's bed-side<sup>33</sup>. By simultaneous recording of cortical-subcortical brain activity (LFP and EEG/MEG) in response to applied emotional-cognitive paradigms, different relationships between brain oscillations and behavior could be established on the basis of time-frequency coupling analyses<sup>34</sup>. In turn, such patterns could lead to prospective biomarkers of a patient's individualized cognitive and emotional states and optimization of treatment parameters considering individualized settings.

The following protocol targets invasive and non-invasive neurophysiological recording in humans for the assessment of cognitive and emotional function, specifically at the cortical and subcortical level (EEG and LFPs).

First, the neurophysiological recording steps illustrated in the video, that accompanies the present protocol, correspond to a recording with an example patient with movement disorder that performs the so called Flanker task (Example 1).

Second, steps in the protocol are discussed by focusing on the methodology of analysis and sample results taken from a published DBS example in chronic DOC<sup>26</sup> (Example 2).

These two examples highlight the applicability of the proposed protocol to DBS-treated patients with different disorders and various experimental paradigms.

## Protocol

The DBS procedure and invasive recordings were approved by the Ethics Commission of the University Clinic Düsseldorf, Germany.

## 1. Experimental Paradigm Design and Patient's Consent

NOTE: Design an experimental paradigm or select an existing experimental paradigm to target a cognitive/emotional aspect of interest.

1. Select patients that will undergo DBS-treatment. Ask if the DBS-Patient meets the study's inclusion criteria. If yes, obtain signed informed consent from patient and/or ethical commission (if applicable) to carry out a post-operative recording and application of the respective cognitive paradigm.

Note: Post-operative recording takes place the following day after an initial DBS surgery is carried out for DBS electrode implantation (together with their corresponding externalization from the head by means of special cables) and before a second surgery takes place regarding permanent implantation of DBS electrodes and stimulator.

1. In the Flanker task (Example 1), obtain signed informed consent from a patient with movement disorder (e.g. Huntington's or Parkinson's disease) in order to carry out a post-operative recording. The goal of the Flanker experiment is to test the patient's ability for adaptation to error behavior and to determine how such adaptation is reflected on brain oscillatory activity at the cortical and subcortical level.

NOTE: The choice of a patient is dictated by the cognitive mechanism to be addressed and the patient's disorder. In the DBS-DOC case-example (Example 2), a female DOC patient who suffered from a head injury at the age of 38 was selected. Because of the patient's condition limiting informed consent, DBS treatment and experimental participation was approved solely by the local ethics commission. The main goal of the DOC postoperative recording was to determine whether brain function in relation to cognitive-emotional processing was still intact in a patient with such severe disorder of consciousness.

2. Choose between the type of stimulus to be presented (auditory, visual). Identify the order of stimulus presentation (block or mixed design). Select the duration of stimulus, inter stimulus interval (ISI) and the number of trials.
  1. As one practical example perform the Flanker task (Example 1, **Figure 1A**), to examine the ability to adapt behavior in response to the commitment of response errors. This task consists of visual stimuli (flanked arrowheads vertically arranged).
  2. Flank the target stimulus (arrowhead in the center) by two adjacent arrows (above and below target) either pointing in the same (compatible) or opposite (incompatible) direction, additionally consider stop trials (circle in the center).
  3. Present the target to the left or right, and ask the participant to press a response button with their left or right thumb. In the stop trials, instruct the participants not to respond. Present flankers 200 msec before target. Display the target for 300 msec and set the response stimulus-interval to 2,000 msec (elapsed time is indicated by a cue tone). Present a total of four blocks of 120 stimuli each in this task. Present compatible (60%), incompatible (20%) and stop-trial (20%) stimuli randomly.

NOTE: This value for the stimulus-interval was chosen to avoid a large number of missed trials when considering motor disabled patients. Flankers and target were switched off simultaneously. Patients were instructed to respond as quickly as possible.

NOTE: In the DBS-DOC case-example (Example 2, **Figure 1B**), the experimental paradigm consisted of neutral non-addressing and familiar-addressing speech stimuli<sup>26</sup> in a block design. The stimulus duration was set-up to 4 sec (with a randomized 4 5 sec inter-stimulus-interval). A total of 80 trials per condition were considered in this paradigm (**Figure 1B**).

3. Envision the patient's physical constraints and needs in a post-operative setting recording. Specifically, determine if the patient is able to make use of the computer keyboard by considering the presence of excessive chorea movements (Huntington's disease) or tremor (Parkinson's disease).
  1. Make sure the patient is able to see the monitor (as the local anesthetic or the stereotactic head frame applied during DBS surgery may have caused swelling in the face and around the eyes) and sit comfortably during the duration of the whole experiment. Do not perform the experiment, if the patient fails to meet these conditions.

## 2. Set-up for Postoperative Subcortical (LFPs) and Surface (EEG) Recordings

1. Set up the EEG equipment (see **Materials** in the supplementary files) in the room where the experiment will be conducted. Connect the recording computer to the EEG system. Start the EEG recording software (see "materials" in the supplementary files).
2. Click "File" and then "New workspace" to define the workspace in the EEG recording software by specifying: a sampling frequency of 5 kHz, a low cut-off (DC) and high cut-off frequency (1,000 Hz), EEG channels according to the international 10/20 system (at least: fronto-central (Fz), centro-central (Cz), fronto-polar reference (Fpz) and ground (mastoid) and depending on the paradigm furthermore parieto-central (Pz), occipito-central (Oz), temporal (T3/T4), fronto-medial (F3/F4), fronto-lateral (F7/F8) ) (**Figure 2D**) and LFP channels (LFPL 0, LFPL1, LFPL2, LFPL3 (left hemisphere, **Figure 2C**); LFPR0, LFPR1, LFPR2 and LFPR3 (right hemisphere)). Click "Monitor" to verify that the specified channels are now set up for recording.  
 NOTE: The preparation beforehand of the workspace is recommended in order to minimize the experiment time and to oversee unexpected changes in the recording's configuration. It is recommended to ensure the highest temporal resolution, correct filter settings, adequate sampling rate and proper selection of channels of interest.
3. Set up the stimulus computer by connecting the parallel port to the EEG system. Start the stimulus software. Click "run" to check the paradigm's functionality on the computer's monitor (visual stimuli) and/or speakers (auditory stimuli, sound cues). Make sure markers (triggers) from the stimulus computer are read into the recording system during presentation of stimuli and subject's response by checking their appearance on the EEG recording software.  
 NOTE: Triggers from stimulus devices must have duration of at least 200  $\mu$ sec to be detected by the EEG system (with the 5 kHz sampling rate). Since triggers are markers of event-related-events or evoked related activity that occur at a specified period of time their function is crucial for posterior data analysis. In the DBS-DOC case-example (Example 2), the experimental paradigm (**Figure 1B**) consisted of auditory stimuli (familiar an unfamiliar voices) so triggers were set up at the beginning and end of each stimuli presented. In the case of the Flanker task (**Figure 1A**) triggers were set up at the instant when 1) the flankers and target stimuli appeared, 2) the patient responded and 3) a cue tone was heard to inform the patient that the response-time had elapsed.
4. Mark the vertex of the patient's head as the midpoint between the nasion and inion by using a skin marker pen and by following the advice of an experienced neurologist or EEG specialist. Additionally, mark chosen EEG electrode positions using the 10-20 system. Attach EEG surface electrodes to the scalp by first cleaning each selected location with an isopropyl alcohol pad and after the use of abrasive paste.  
 NOTE: Such actions are constrained by the placement of bandages on the head of the DBS patient. However, an experienced neurologist should be able to define an appropriate (approximate) location for each electrode/channel. To ensure proper contact move hair out of the way (if applicable). The use of self-adhesive electrodes secured by surgical tape might be used due to easiness of placement.
5. Connect externalized DBS electrodes to a percutaneous extension. Connect percutaneous extension to external cable connector. Connect each electrode provided by the external cable connector to the EEG control box according to the EEG recording set-up. Connect EEG scalp electrodes to the EEG control box by first plugging ground and reference.
6. Attach EMG electrodes (reference and active electrodes) at specified muscles by first cleaning the area with an isopropyl alcohol pad. Connect EMG electrodes to EEG control box.  
 NOTE: This step is optional and mainly conducted when motor tasks are considered into the paradigm or when it is required to monitor the activity of muscles as in the case of patients with motor disorder.
7. Click "Monitor" to visualize data. Make sure EEG and EMG signals displayed on the monitor are artifact-free by detecting the presence of jittering and superimposed high frequency components. Check guidelines about types of artifacts and other factors related to recording electroencephalographic signals<sup>35</sup> and/or request technical advice from an experienced neurologist or neuroscientist until you become familiar with the type of disturbances present in such physiological recordings.  
 NOTE: This step is important to ensure high quality signals for off-line data analysis.

## 3. Recording of Post-operative Subcortical (LFPs) and Surface (EEG) Brain Activity

1. Provide instructions to the patient. Make sure the patient is comfortable and instruct him/her to stop the experiment at any time of discomfort.
2. Click "run" on the stimulus software so that the patient is able to see the paradigm on the monitor and/or listen to the cue tones and sounds. Perform a training session with the patient until he/she is comfortable with the task. Start simultaneous recording of subcortical (LFP) and cortical (EEG) brain activity while the patient performs the experimental task.  
 NOTE: In the case of the DBS-DOC case example (Example 2) the paradigm consisted of auditory stimuli in a block design as described in (**Figure 1B**). In the case of the Flanker task (**Figure 1A**), visual stimuli corresponding to three conditions (compatible (60%), incompatible (20%) and stop-trial (20%)) were presented randomly within each block (mixed design), each block consisted of 120 stimuli and the paradigm consisted of a total of four blocks. After the task has been finalized, data is stored on the hard disk of the recording computer for later off-line screening and quantitative analysis.

## 4. Data Analysis

NOTE: Steps by using EEG analysis software:

1. Open the EEG analysis software (see "materials" in the supplementary files) and click "New" to visualize the recorded data by specifying the folder paths (raw, history and export) and data's name. Click "Edit channels" to select channels of interest. Rename channels if necessary.

2. Click "Channel Preprocessing" and then "New Reference" to re-reference adjacent DBS contacts and thus create virtual bipolar contacts for left and right hemispheres. Repeat this process to create a virtual montage for EEG channels.  
NOTE: A bipolar re-reference montage is important to minimize volume conduction effects and to improve spatial reliability of the recorded signals. In the case of the DBS-DOC case example (Example 2), the following bipolar channels were set-up DBS: LFPL01, LFPL12, LFPL23, LFPR01, LFPR12, LFPR23 and EEG: Cz/Fz, Pz/Cz, Oz/Pz, T3/Cz and T4/Cz. It is worthy to emphasize that while MEG recorded signals are reference-free, EEG signals need to be referenced to set true non-arbitrary zero value signals in a common framework. Existing EEG reference systems include: Cz or FPz reference, average between electrodes on the two ears, average reference (considering all of the channels), two- or single-mastoid reference and noise reference. For the purpose of data analysis, different re-reference arrangements can be utilized, for instance bipolar contacts are appropriate when targeting time-frequency coupling analysis between DBS and EEG signals.
3. Click "raw data inspection" to screen data for physiological and equipment related artifacts with emphasis on motor jittering and equipment disturbances. Mark segments in which artifacts are present.  
NOTE: When recording scalp activity and simultaneously subcortical activity through DBS externalized leads, EEG appears more robust to noise artifacts than techniques such as MEG for which current efforts are being directed towards improving signal to noise ratio. Due that patients with motor disorders suffer from involuntary movements such as chorea and tremor the appearance of motor jittering artifacts in the recorded signals needs to be accounted for. Other disturbances are due to eye blinks and equipment related artifacts. Focusing on the DBS-DOC case example (Example 2), artifact inspection was performed by visual examination and artifacts were manually marked. The sole application of an automatic artifact inspection mode is discouraged as some artifacts may not be recognized by a specified criterion.
4. Click "Data Filtering" and then "IIR Filters" to specify a notch filter: 50Hz (dealing with power line artifacts) and Butterworth Zero Phase Filters by specifying Low and High Cutoff parameters. Click "Change Sampling Rate" to downsample the recorded signals to a specified frequency and also specify the interpolation type.
  1. In the DBS-DOC example; set Low Cutoff: 1.0000 Hz, Time constant: 0.1592s, slope: 48 dB/oct; High Cutoff: 80.0000 Hz, Time constant: 0.1592 sec and 48 dB/oct and downsampling frequency to 512 Hz by using spline interpolation.  
NOTE: Optionally, perform filtering by customized scripts based on well-known open source suites: Fieldtrip (<http://www.fieldtriptoolbox.org/>), EEGLab (<http://scn.ucsd.edu/eeglab/>) and SPM8 (<http://www.fil.ion.ucl.ac.uk/spm/software/spm8/>). In the case of the first, sample scripts are provided in (<http://www.fieldtriptoolbox.org/tutorial/preprocessing>). Other suites also provide detailed documentation to carry out this step.  
NOTE: Down-sampling at any point will limit the frequency space that is available for further analysis according to the Nyquist theorem. Considering the DBS-DOC case-example, the selected sampling frequency of 512 Hz is appropriate when considering a frequency band up to 80 Hz.  
NOTE: Alternatively, perform down-sampling by customized scripts based on well-known open source suites: Fieldtrip (<http://www.fieldtriptoolbox.org/>), EEGLab (<http://scn.ucsd.edu/eeglab/>) and SPM8 (<http://www.fil.ion.ucl.ac.uk/spm/software/spm8/>). In the case of the first, script examples are provided (<http://www.fieldtriptoolbox.org/tutorial/preprocessing>). Other suites also provide documentation to carry out this step.
5. Export bipolar channels of interest by clicking "Export" and then "Generic Data". Export data markers (triggers) by clicking "Export" and then "Markers". Name the files to be exported by selecting a "txt" format.  
NOTE: In order to use the Fieldtrip toolbox in the next steps it is suggested to export channels in (.txt) multiplexed format and also recommended to include a "vmrk" file that includes info about exported channels. It is also suggested to use a (.txt) format for the exported markers while the option of skipping markers corresponding to bad intervals selected in step 4) is offered.

NOTE: Steps by using Fieldtrip:

6. Start-up MATLAB and click on "set path" to add the Fieldtrip folder's path in case it is not done by default.
7. Put the data previously pre-processed and markers into a cell-array-structure that is compatible with the functions within Fieldtrip by running ([Script 1-Supplementary File](#)) without missing to specify: The directory that contains the EEG and LFP files from step 7, channel names, sampling frequency, sample time, trials. (Optionally) Perform artifact rejection by "uncomment" the indicated code. This script saves the data into a specified file that will be used in the next steps.
8. Calculate LFP's spectral power for channels of interest by running ([Script 2-Supplementary File](#)) without missing to specify: the directory that contains the file generated by (Script 1), the method (wavelet or mtmconvol), the width of the window, the frequency of interest (foi), time's period of interest (toi), and frequency baseline correction (optional). Define the type of statistical analysis and desired p-value.  
Note: In the DBS-DOC case-example (Example 2), power analysis was performed by considering a stimulus-locked wavelet time frequency analysis (Morlet wavelet (width = 5)) with Hanning taper, a frequency range of 4-80 Hz and a time period between -1 to 4 sec. Due that wavelets have variable resolution in time and frequency. When selecting a wavelet, we decide a trade-off between temporal and spectral resolution. In particular, Morlet wavelets possess a sinusoidal shape weighted by a Gaussian kernel that enables capturing local oscillatory components in a time series. Making the width parameter smaller will increase the temporal resolution at the expense of frequency resolution and vice versa. The spectral bandwidth at a given frequency F is equal to  $F/\text{width} \times 2$  (for F = 40 Hz and width = 5 the spectral bandwidth is 16 Hz) while the wavelet duration is equal to  $\text{width}/F/\pi$  (for F=40 Hz and width=5 the wavelet duration is 39.8 msec). A cluster based (time and frequency variables) randomization approach was used for statistical analysis between conditions (p-level of .05 in a two-sided test)<sup>39</sup>. As an example of the output obtained by performing this step please look at **Figure 4A** and **Figure 4D**. Time-frequency response analysis was performed by customized scripts based on the open source software Fieldtrip (<http://www.fieldtriptoolbox.org/>). Specific details about how to customize a script to accomplish this step can be found in [http://www.fieldtriptoolbox.org/reference/ft\\_freqanalysis](http://www.fieldtriptoolbox.org/reference/ft_freqanalysis).
9. Calculate coherence between subcortical and cortical signals by running ([Script 3-Supplementary File](#)) without forgetting to specify: segments length, overlap percentage, frequency of interest. As for the statistical analysis specify the type of analysis and desired p-value.  
Note: Coherence analysis measures the linear relationship between two time series with a constant ratio of amplitudes<sup>40</sup>. In the DBS-DOC case-example (Example 2), segments of 1 sec with 50% overlap were used for the calculation of coherence by focusing on the frequency interval between 1 and 25 Hz. A cluster-based (time and frequency variables) randomization approach was used for within-subject analysis of coherence (p-level of .05 in a two-sided test)<sup>41</sup>. Furthermore, the imaginary part of coherence was computed<sup>42</sup>. The basic steps to customize a script for coherence analysis are described in (<http://www.fieldtriptoolbox.org/tutorial/coherence>). As an example of the output obtained by performing this step please look at **Figure 4B**.

10. Calculate cross frequency phase amplitude coupling (PAC) by running the software implementation available as supplementary file in reference<sup>43</sup>.

Note: In the DBS-DOC case example (Example 2), cross-frequency analysis PAC was calculated by using the entire free-artifact recording for different combinations of bipolar channels. In particular, normalized direct PAC (ndPAC)<sup>43</sup> was preferred because it enabled determination of significant coupling at different statistical levels while setting-up to zero the non-significant couplings (p-level: 0.1). As a result, frequency ranges for phase and amplitude coupling could be selected on the basis of their significance. In the DBS-DOC case example, the phase frequency range considered was 3-22 Hz while the amplitude frequency range was set up to 35-80 Hz. The LFP-EEG channels selected for PAC analysis were LFPR23 and EEGFzPz on the basis of the coherence analysis performed in step 5.5. As an example of the output obtained by performing this step please look at **Figure 4C**.

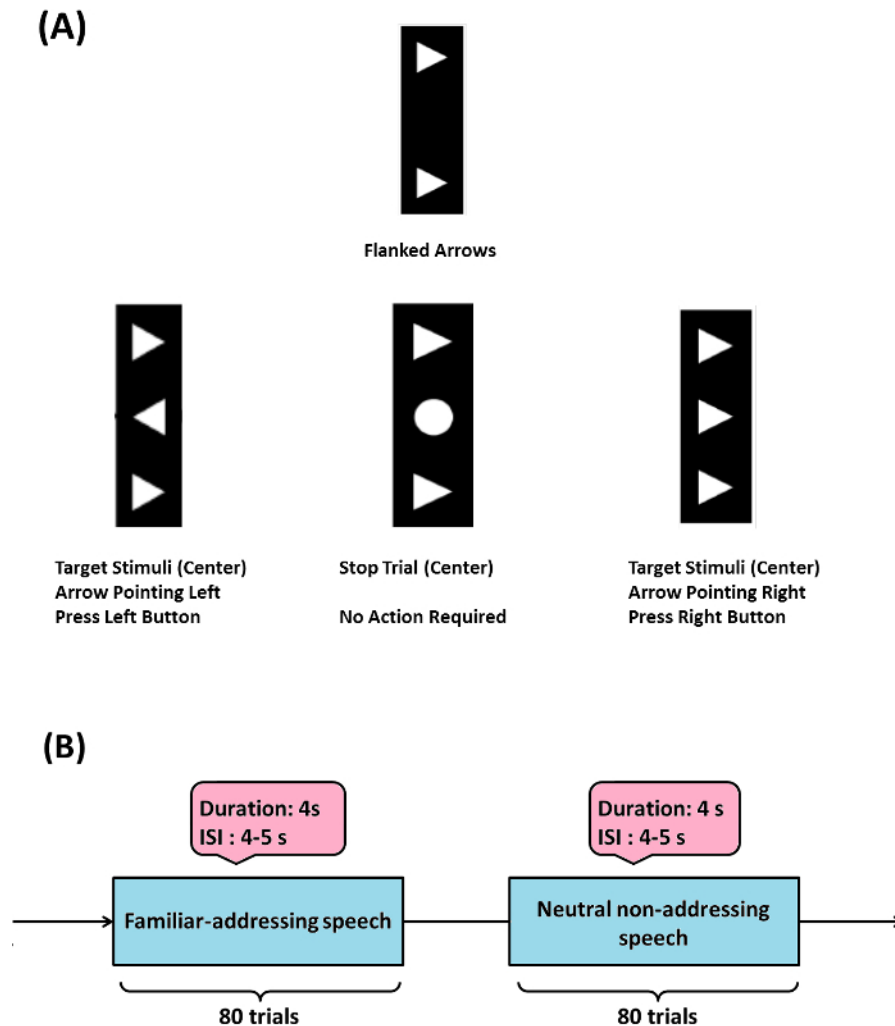


**Figure 1: Sample Experimental Paradigms.** (A) (Example 1) Flanker task: target stimulus (arrowhead in the center) is flanked by two adjacent arrows (above and below target) either pointing in the same (compatible) or opposite (incompatible) direction, stop trials (circle in the center) were also considered. When target is pointed to the left or right, a participant has to press a response button with their left or right thumb respectively, in the stop trials participants are instructed not to respond. The Flanker task used here was modified from the initially programmed version by Prof. C. Beste and his group (please see acknowledgements). (B) (Example 2) emotional-cognitive speech paradigm used in the DBS-DOC case-example. [Please click here to view a larger version of this figure.](#)

## Representative Results

For the DBS-DOC case (Example 2), we now provide data on target localization for DBS implantation, schematic diagrams of LFP electrode and EEG set up, exemplary recordings of EEG and LFP activity (raw data) and representative analysis results:

**Figure 2A** shows planned trajectory (black line) projected on an anatomic atlas<sup>36</sup>, section 30, coronary, 10.7 mm behind the anterior commissure (AC) (red line: AC-PC plane). Red circles mark targeted areas of the lowermost 15 mm (atlas grid size: 10 mm) with iml = internal medullary lamina thalami and Rt = reticular thalamic nucleus. VA = ventroanterior thalamic nucleus, AV = anteroventral thalamic nucleus, AM = anteromedial thalamic nucleus, Fa = fasciculus nucleus, lthA = interthalamic adhesion.



**Figure 2B** shows the final electrode in the central thalamus visualized on a 3D atlas<sup>37</sup>. Two orthogonal planes of section along the axis of the electrode in the right hemisphere after registration of the 3D atlas with the CT scan by means of the atlas<sup>38</sup>. The four contacts of the electrode (blue circles) were located in the right thalamus (R-Thal). GPI = internal globus pallidus, STN = subthalamic nucleus, ZI = zona incerta, RPT = reticular perithalamic nucleus, RN = red nucleus.

**Figure 2C** shows a schematic drawing of the DBS electrode. Electrode contacts were re-referenced offline, resulting in three bipolar LFP channels for each hemisphere (LFPL01, LFPL12, LFPL23, LFPR01, LFPR12, and LFPR23). EEG electrode montage (10-20 system) with electrodes used during recording in the DOC case-example (Fz, Cz, Pz, Oz, T4, T3 and Fpz) (**Figure 2D**)

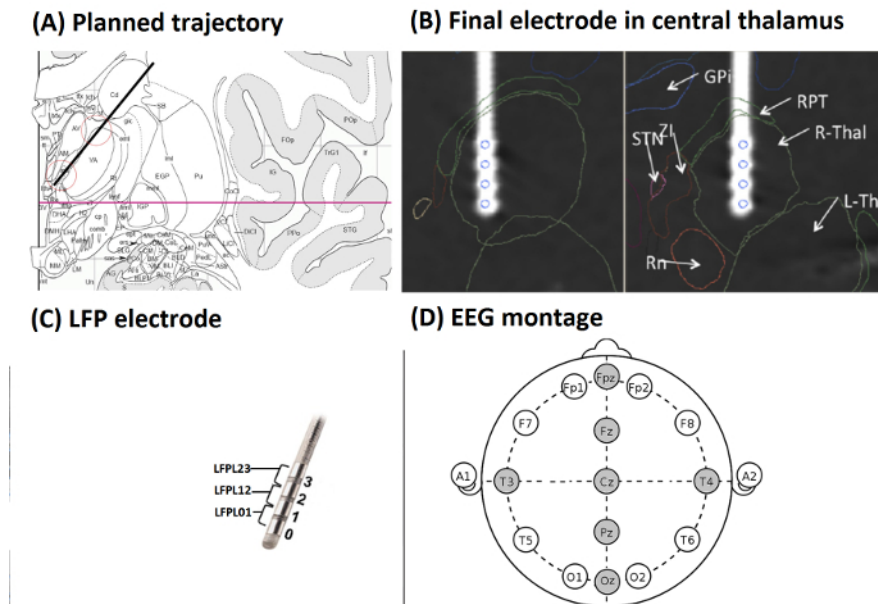


**Figure 2: Target Localization, LFP Electrode and EEG Set-up (from Example 2).** (A) Planned trajectory (black line) projected on an anatomic atlas<sup>36</sup>, section 30, coronary, 10.7 mm behind AC (red line: AC-PC plane). Red circles mark targeted areas of the lowermost 15 mm (atlas grid size: 10 mm) with iml = internal medullary lamina thalami and Rt = reticular thalamic nucleus. VA = ventroanterior thalamic nucleus, AV = anteroventral thalamic nucleus, AM = anteromedial thalamic nucleus, Fa = fasciculosus nucleus, lthA = interthalamic adhesion. (B) Final electrode in the central thalamus visualized on a 3D atlas<sup>37</sup>. Two orthogonal planes of section along the axis of the electrode in the right hemisphere after registration of the 3D atlas with the CT scan by means of an atlas<sup>38</sup>. The four contacts of the electrode (blue circles) were located in the right thalamus (R-Thal). GPI = internal globus pallidus, STN = subthalamic nucleus, ZI = zona incerta, RPT = reticular perithalamic nucleus, RN = red nucleus. (C) Schematic drawing of the DBS electrode. Electrode contacts were re-referenced offline, resulting in three bipolar LFP channels for each hemisphere. (D) EEG electrode montage (10 - 20 system) with electrodes used in the DOC case-example highlighted in gray. (Figures A and B were modified with permission from<sup>26</sup>, Figure C was modified with permission from Medtronic). [Please click here to view a larger version of this figure.](#)

**Figure 3A** shows exemplary EEG recordings corresponding to bipolar channels: T4Cz, T3Cz, PzCz, OzPz and FzPz in the case of the neutral non-addressing condition (left) and the familiar addressing condition (right).

**Figure 3B** displays exemplary LFP recordings corresponding to bipolar channels: LFPL23 and LFPR23 in the case of the non-addressing condition (left) and the familiar addressing condition (right).

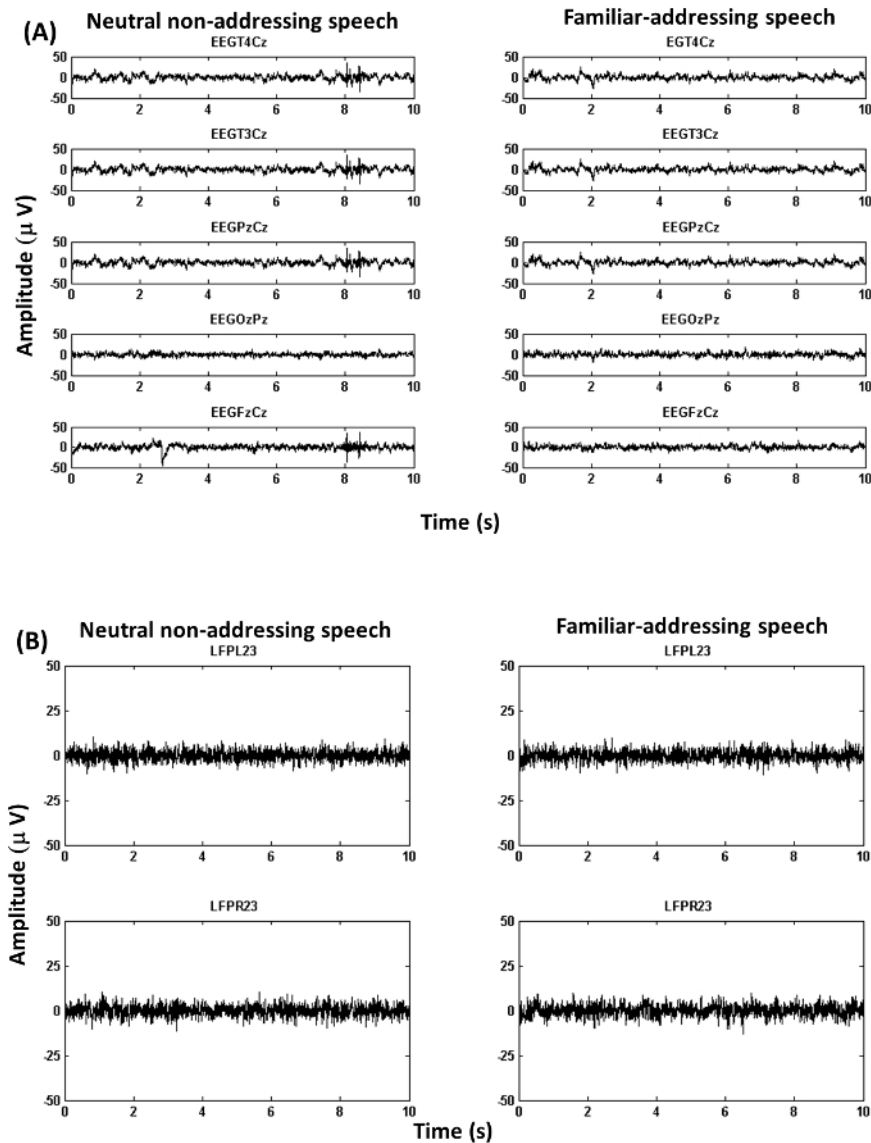


**Figure 3: Exemplary Recordings (from Example 2).** (A) Figure shows EEG recordings. The figure illustrates EEG traces corresponding to bipolar channels (see 4.2 for details about channel re-referencing). (B) Figure shows LFP recordings. The figure illustrates LFP traces corresponding to bipolar channels in the case of left and right hemispheres (see 4.2 for details about channel re-referencing). [Please click here to view a larger version of this figure.](#)

Analysis of stimulus-locked modulation of oscillatory activity within central thalamus revealed a right-sided significant ( $p = 0.044$ ) increase of beta power (12-25 Hz) within the first second (0.45-0.55 sec) when contrasting neutral addressing vs. familiar-addressing conditions (**Figure 4A**).

Coherence analysis between channels PzCz (EEG) and LFPR23 (right hemisphere) revealed a significant difference between conditions in the theta band. Also, the imaginary part of coherence showed deviation from zero indicating a phase delay between LFP and EEG (**Figure 4B**). Local analysis revealed significant ( $p = 0.01$ ) theta-gamma PAC (with max. at 5-to-75 Hz) for the right local LFP channel (LFPR23-LFPR23) in the familiar-addressing condition (**Figure 4C**).

Analysis of power change corresponding to LFPR23 revealed an early beta increase within the first second (green box) and a late theta modulation (red box) (**Figure 4D**, Top). It is also noticeable that Gamma around 40 Hz (green circle/ellipse) is followed by a broader and higher gamma up to 80 Hz (**Figure 4D**, Top). A significant theta increase in the familiar-addressing condition at 4-6.5 Hz and time period 2.6-2.8 sec (red circle), ( $p = 0.048$ ) on LFPL23 as well as an increased trend on LFPR23 were revealed (**Figure 4D**, Bottom).

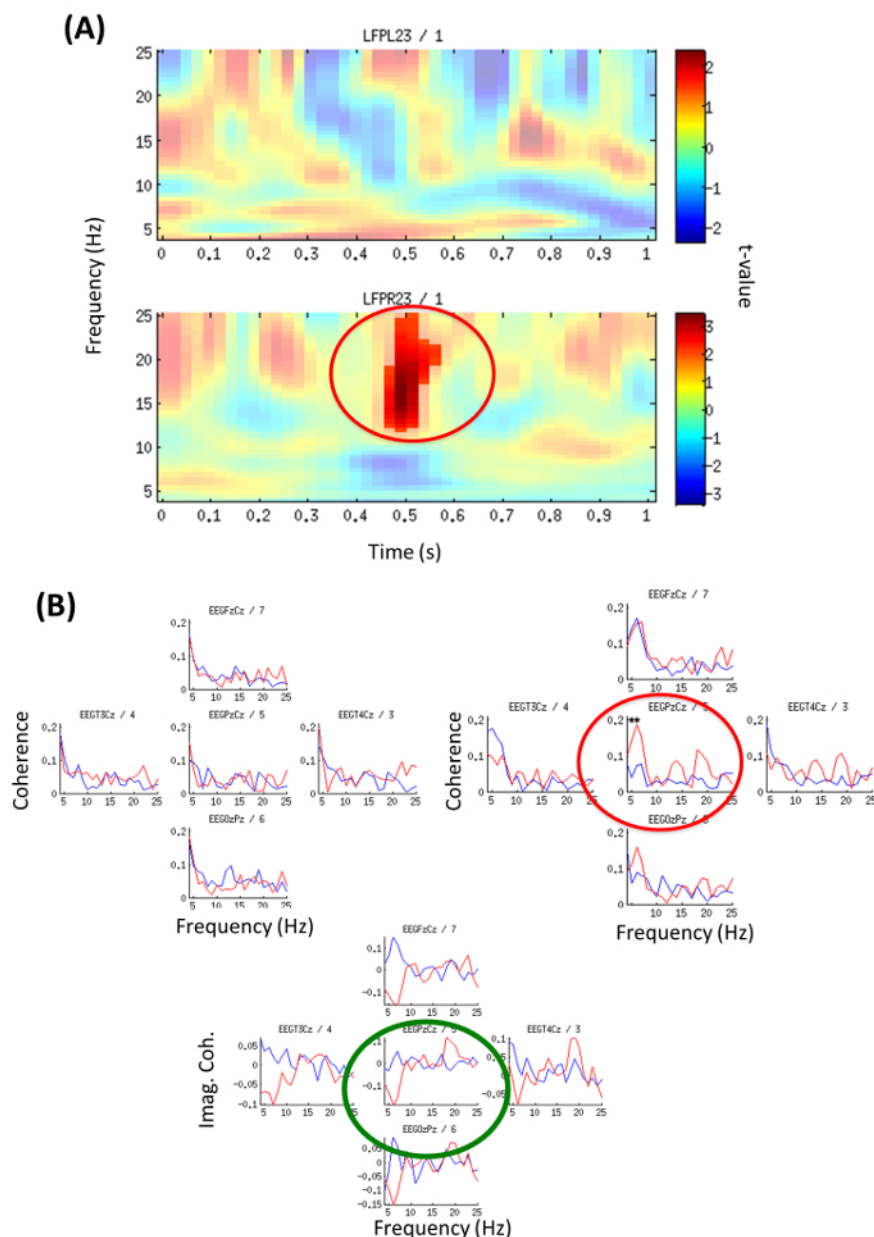


**Figure 4: Time-frequency Power Analysis and EEG-LFP Coherence (from Example 2).** (A) Local oscillatory power contrasting neutral versus familiar-addressing condition for the first second; Color code represents t-values. Top: left channel LFPL23; Bottom: right channel LFPR23. Significant beta increase ( $p = 0.044$ ) at 12-25 Hz, 0.45-0.55 sec (red circle). (Modified with permission from<sup>26</sup>). (B) Familiar-addressing condition (red line) and neutral non-addressing condition (blue line). Coherence was calculated on independent 1 sec segments from epochs with duration 0-4 sec and averaged across all segments. Top (left): Coherence with channel LFPL23 left hemisphere, Top (right): Coherence with channel LFPR23 right hemisphere. Significant difference between conditions ( $p = 0.044$ ) is indicated by red circle/stars for coherence with channel PzCz, 5-6 Hz. Bottom: Imaginary part of coherence between LFPR23 right hemisphere and channel Cz (green circle) shows deviation from zero meaning a phase delay between LFP and EEG (thus effect not due to volume conduction). (Modified with permission from<sup>26</sup>) [Please click here to view a larger version of this figure.](#)



(C)

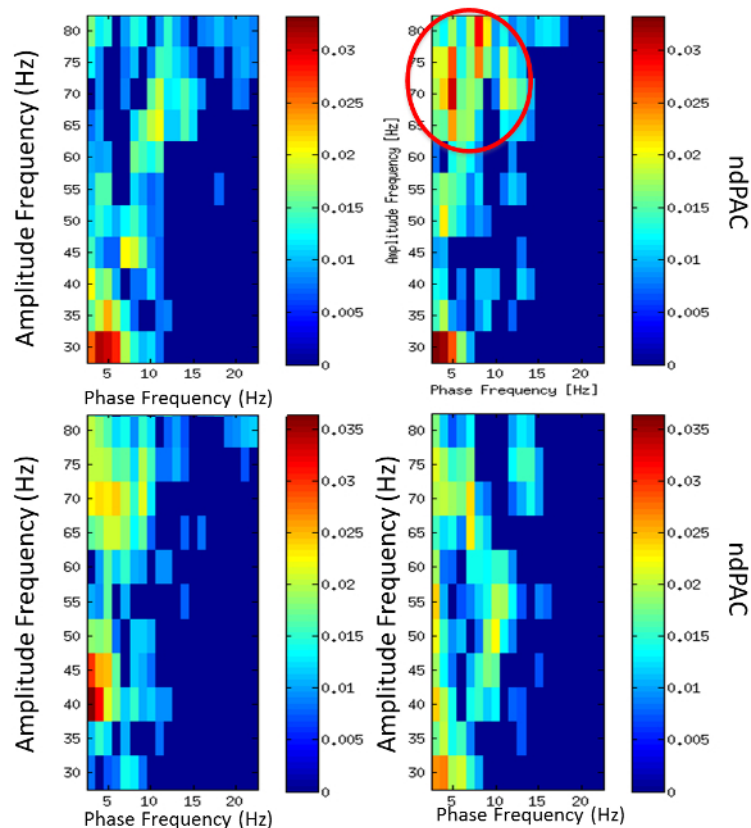


**Figure 4C: Phase Amplitude Coupling (PAC) (from Example 2).** PAC for phase frequencies 3-22 Hz and amplitude frequencies 35-80 Hz. Colors encode normalized direct phase-amplitude cross-frequency coupling (ndPAC). Spurious coupling is set to 0 ( $p = 0.01$ ). Conditions: left: neutral, right: familiar-addressing. Top: PAC of right local LFP channel LFPR23-LFPR23 showing PAC in familiar addressing condition with max. at 5-75 Hz (red circle). Bottom: PAC of right LFP-EEG combination with LFPR23-EEGPzCz. (Modified with permission from<sup>26</sup>) [Please click here to view a larger version of this figure.](#)

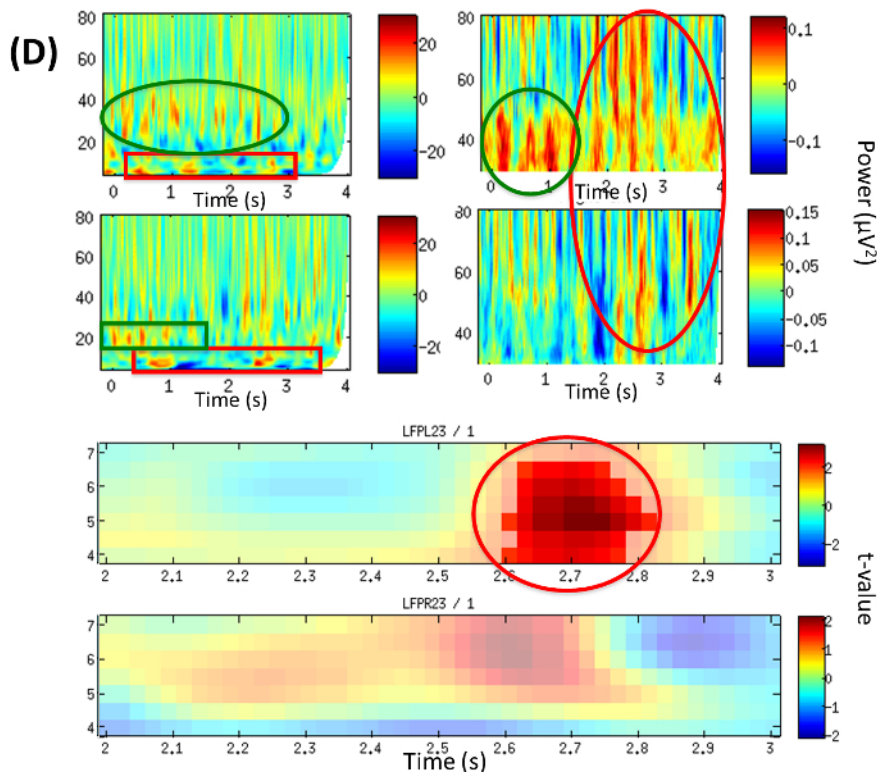


**Figure 4D: LFP Time-frequency Analysis (from Example 2).** Time frequency plots of local power changes at LFP23. TOP: Power difference from baseline in the familiar-addressing condition over the period of the trial (0-4 sec). Left: broad frequency band 5-80 Hz, right: gamma band; top row: left hemisphere (LFPL23), bottom row: right hemisphere (LFPR23). BOTTOM: Statistical contrast between conditions illustrating significant theta increase in the familiar-addressing condition at 4-6.5 Hz and time period 2.6-2.8 sec (red circle),  $p = 0.048$  on LFPL23 and increase (trend) on LFPR23. Color map encodes t-values; top: left hemisphere (LFPL23), bottom: right hemisphere (LFPR23). (Modified with permission from<sup>26</sup>) [Please click here to view a larger version of this figure.](#)

## Discussion

In contrast to non-invasive brain recording techniques like scalp-EEG and MEG, the proposed combined invasive and non-invasive neurophysiological recording framework provides a remarkable opportunity to extract information from cortical and subcortical areas in relation to cognitive-emotional tasks. Such information is reflected by brain oscillatory activity at multiple frequency bands and different levels of organization in relation to brain functioning<sup>44</sup>. Brain oscillatory patterns that are relevant in our recording framework include: subcortical oscillatory activity (LFPs), changes in cortical-subcortical coherence indicating changes in linear correlation between activities at cortical and subcortical regions on specific frequency bands, subcortical phase-amplitude coupling (PAC) and phase-phase coupling (PPC). In particular, the relevance of PAC and PPC is emphasized as the relation and interaction between oscillations in different frequency bands has been shown to be useful in understanding brain function. In the case of PAC, the phase of a low frequency oscillation is related to the power of a high frequency oscillation thus resulting in synchronization of the amplitude envelope of faster rhythms with the phase of slower rhythms. PPC represents an amplitude independent phase locking between  $n$  cycles of high frequency oscillation and  $m$  cycles of a lower frequency one<sup>45</sup>. Focusing on the DBS-DOC case example (Example 2), analysis of cortical/subcortical recorded data for the familiar-addressing speech condition revealed modulation of oscillatory activity in the beta and theta band within the central thalamus together with increased thalamocortical coherence in the theta band. In addition, a theta phase - gamma amplitude coupling was apparent within the thalamus locally. These findings not only support the involvement of the thalamus in emotional and cognitive processing but also emphasize functions that are intact in chronic DOC patients and that could be useful in the assessment of conscious states in such patients<sup>26</sup>.

Methodologically, as exemplified by our two examples, the most relevant steps for recording and analysis of cortical-subcortical brain activity in relation to emotional-cognitive processing include:

- 1) Design of an experimental paradigm, by taking into consideration the patient needs and constraints in a post-operative setting, ensuring that he/she will be able to carry out the task specified in the study without compromising his/her integrity while maximizing the chance of success in the completion of the experiment.
- 2) Obtaining signed informed consent from patient, patient's family members or ethical commission to carry out post-operative recording. In the DBS-DOC case example (Example 2) approval was solely obtained from the ethical commission due to the patient's unconscious state (coma). In the case of patients with motor disorders consent was obtained directly from the patient.
- 3) Definition of an appropriate experimental set-up for simultaneous recording of subcortical LFPs and cortical M(EEG) activity. In the case of EEG, we emphasize: Proper choice and set-up of an EEG channel montage and electrode placement on the patient's scalp. In particular, electrode placement could be challenging due to the presence of bandages on the patient's head after DBS surgery, so advice of an EEG

professional or neurologist is highly recommended for appropriate placement; It is recommended not to carry out any impedance control check in order to prevent any current to be sent directly into the brain of the patient ("off-label" use of EEG-amplifier). Note that the impedance check's mode in many EEG systems utilizes a small current that passes through all attached electrodes so the resulting voltage and impedances are estimated by Ohm's law; Selection of an appropriate recording sampling rate and frequency band is mainly determined by factors such as the EEG equipment capabilities, the research question under study and the Nyquist sampling rule, which states that the sampling rate required to eliminate alias frequencies in a bandwidth limited signal (at a value equal to half the Nyquist rate) is two times the highest frequency component present in the signal.

4) Selection of appropriate software tools: All the calculations in the quantitative analysis of the DBS-DOC data (Example 2) were performed by commercial analysis software, open source suites<sup>46</sup> and self-customized scripts (see supplementary files). An advantage of open source software tools is the opportunity to customize one's own analysis pipelines by modifying and combining existing scripts (under the common license attribution). However, in order to do so deeper understanding of the mathematical basis of signal processing and programming are required. Also, data processed by such customized pipeline need to comply with the format required by the specific suite. In the case of commercial software tools, data processing is facilitated by graphical interfaces that make each processing step as intuitive as possible, however users are limited in their capability to modify the algorithms included in the software. As exemplified by the present protocol, a combination of commercial and open source software tools is fruitful as long as the data can be exported (imported) in a compatible way from one system to the other.

5) Limitations and Modifications: The proposed invasive/non-invasive recording framework has limitations in both its use and the recordings provided. As a clinical technique, it is only directed to patients that undergo DBS treatment for a specific medical condition and brain target, consequently the brain areas considered for study will be constrained by the operative plan. The spatial resolution of recordings provided by this technique is at the level of LFP potentials, thus medical translational studies requiring analysis of brain activity at the multiscale level will have to be complemented by animal studies involving recordings at the single cell level. With regard to the DBS-DOC case-example (Example 2), a limitation pertains also to the generalizability of the obtained results as it deals with a single-case study.

Possible modifications and troubleshooting of the Flanker task (Example 1) include enlargement of the response stimulus-interval (>2,000 msec) concerning the inability of patients to react within a specified time interval. This is particularly important in the case of Huntington disease patients, who are characterized by jerky involuntary movements together with cognitive and emotional decline. Also, the task (originally consisting of four blocks of 120 stimuli each) may be shortened due to inability of a patient to continue because of fatigue. In this respect, the physical condition and age would be determinant factors for patient's selection.

It is concluded that the proposed invasive/non-invasive brain recording approach not only represents a powerful tool for extracting brain oscillatory patterns at the cortico-subcortical level in relation to cognitive and emotion paradigms, but also stresses the importance of time-frequency-phase analyses for extracting brain synchronization patterns at different spatial and temporal resolutions. Future application of this technique includes the study of cortico-subcortical neural correlates of cognitive and sensory processing by targeting not only patients suffering from motor disorders but also psychiatric disorders such as DOC, OCD, depression and dementia.

## Disclosures

The authors declare that they have no competing financial interests.

## Acknowledgements

This work was supported by ERA-NET NEURON/BMBF Germany (TYMON). Publication fees are covered by a grant from the University Hospital Düsseldorf. The Flanker task used here was modified from the initially programmed version by Prof. C. Beste and his group<sup>47</sup>.

## References

1. Foerster, O., & Altenburger, H. Elektrobiologische Vorgänge an der menschlichen Hirnrinde. *Dtsch. Zschr. Nervenheilk.* **135**, 277-288 (1934).
2. Spiegel, E.A., Wycis, H.T., Marks, M., & Lee A.J. Stereotaxic apparatus for operations on the human brain. *Science*. **106**, 349-350 (1947).
3. Okun, M.S. Deep-Brain Stimulation for Parkinson's disease. *N. Engl. J. Med.* **367**, 1529-1538 (2012).
4. Groiss, S.J., Wojtecki, L., Südmeyer, M., & Schnitzler, A. Deep Brain Stimulation in Parkinson's disease. *Ther. Adv. Neurol. Disord.* **2**, (6), 20-28 (2009).
5. Kalia, S.K., Sankar, T., & Lozano, A.M. Deep brain stimulation for Parkinson's disease and other movement disorders, *Curr. Opin. Neurol.* **26**, (4), 374-80 (2013).
6. Della Flora, E., Perera, C.L., Cameron, A.L., & Madder, G.J. Deep brain stimulation for essential tremor: a systematic review. *Mov. Disord.* **25**, (11), 1550-1559 (2010).
7. Volkmann, J., & Benecke, R. Deep brain stimulation for dystonia: patient selection and evaluation [Review]. *Mov. Disord.* **17**, (3), 112-5 (2002).
8. Hu, W., & Stead, M. Deep brain stimulation for dystonia. *Transl. Neurodegener.* **21**, 3(1), 2 (2014).
9. Mentzel, C.L., Tenback, D.E., Tijssen, M.A., Visser-Vandewalle, V.E., & van Harten, P.N. Efficacy and safety of deep brain stimulation in patients with medication-induced tardive dyskinesia and/or dystonia: a systematic review. *J. Clin. Psychiatry.* **73**, (11), 1434-8 (2012).
10. Huys, D., et al. Management and outcome of pallidal deep brain stimulation in severe Huntington's disease. *Fortschr. Neurol. Psychiatry.* **81**, 202-205 (2013).
11. Hartmann, C.J., Groiss S.J., Vesper J., Schnitzler, A., Wojtecki, L. Brain Stimulation in Huntington's disease. *Neurodegener. Dis. Manag.* In press (2016).
12. Morishita, T., Fayad, S.M., Higuchi, M.A., Nestor, K.A., & Foote, K.D. Deep brain stimulation for treatment-resistant depression: systematic review of clinical outcomes. *Neurotherapeutics.* **11**, (3), 475-84 (2014).

13. Lakhan, S.E., & Callaway, E. Deep brain stimulation for obsessive-compulsive disorder and treatment-resistant depression: systematic review. *BMC Res. Notes*. **4**, 3, 60 (2010).
14. Luigjes, J., et al. Deep brain stimulation in addiction: a review of potential brain targets. *Mol. Psychiatry*. **17**, 572-583 (2012).
15. Hardenacke, K., et al. Deep brain stimulation as a tool for improving cognitive functioning in Alzheimer's dementia: a systematic review. *Front. Psychiatry*. **4**, 159 (2013).
16. Laxton, A.W., Stone, S., & Lozano, A.M. The Neurosurgical Treatment of Alzheimer's Disease: A Review. *Stereotact. Funct. Neurosurg.* **92**, 269-281 (2014).
17. Schrock, L.E., et al. Tourette syndrome deep brain stimulation: A review and updated recommendations. *Mov. Disord.* **30**, (4), 448-471 (2015).
18. Schiff, N.D., et al. Behavioral improvements with thalamic stimulation after severe traumatic brain injury. *Nature*. **448**, 600-603 (2007).
19. Yamamoto, T., & Katayama, Y. Deep brain stimulation therapy for the vegetative state. *Neuropsychol. Rehabil.* **15**, 406-413 (2005).
20. Yamamoto, T., Kobayashi, K., Kasai, M., Oshima, H., Fukaya, C., & Katayama, Y. DBS therapy for the vegetative state and minimally conscious state. *Acta Neurochir. Suppl.* **93**, 101-104 (2005).
21. Lipsman, N., Giacobbe, P., & Lozano, A.M. Deep brain stimulation in obsessive-compulsive disorder: neurocircuitry and clinical experience. *Handb. Clin. Neurol.* **116**, 245-50 (2013).
22. Mallet, L. et al. Stimulation of subterritories of the subthalamic nucleus reveals its role in the integration of the emotional and motor aspects of behavior. *Proc. Natl. Acad. Sci. USA*. **104**, (25), 10661-10666 (2007).
23. Rotge, J.Y., et al. A challenging task for assessment of checking behaviors in obsessive-compulsive disorder. *Acta Psychiatr. Scand.* **117**, (6), 465-473 (2008).
24. Clair, A.H., et al. Excessive checking for non-anxiogenic stimuli in obsessive-compulsive disorder. *Eur. Psychiatry*. **28**, (8), 507-13 (2013).
25. Burbaud, P., et al. Neuronal activity correlated with checking behaviour in the subthalamic nucleus of patients with obsessive-compulsive disorder. *Brain*. **136**, 304-17 (2013).
26. Wojtecki, L., et al. Modulation of central thalamic oscillations during emotional-cognitive processing in chronic disorder of consciousness. *Cortex*. **60**, 94-102 (2014).
27. Menon, D.K., et al. Cortical processing in persistent vegetative state, Wolfson Brain Imaging Centre Team. *Lancet*. **352**, 200 (1998).
28. Monti, M.M., et al. Willful modulation of brain activity in disorders of consciousness. *New. Engl. J. Med.* **362**, 579e589 (2010).
29. Owen, A.M., Coleman, M.R., Boly, M., Davis, M.H., Laureys, S., & Pickard, J.D. Detecting awareness in the vegetative state. *Science*. **313**, 1402 (2006).
30. Hirschmann, J., et al. A direct relationship between oscillatory subthalamic nucleus-cortex coupling and rest tremor in Parkinson's disease. *Brain*. **136**, 3659-70 (2013).
31. Hirschmann, J., et al. Differential modulation of STN-cortical and cortico-muscular coherence by movement and levodopa in Parkinson's disease. *Neuroimage*. **68**, 203-13 (2013).
32. Okada, Y., Lähteenmäki, A., & Xu, C. Experimental analysis of distortion of magnetoencephalography signals by the skull. *Clin. Neurophysiol.* **110**, 230-238 (1999).
33. Vaughan, T.M., McFarland, D.J., & Schalk, G. The Wadsworth BCI Research and Development Program: at home with BCI. *IEEE Trans. Neural Syst. Rehabil. Eng.* **14**, 229-33 (2006).
34. Gross, J. Analytical methods and experimental approaches for electrophysiological studies of brain oscillations. *J. Neurosci. Methods*. **228**, 57-66 (2014).
35. Pivik, R.T., Broughton, R.J., Coppola, R., Davidson, R.J., Fox, N., & Nuwer, M.R. Guidelines for the recording and quantitative analysis of electroencephalographic activity in research contexts. *Psychophysiology*. **30**, 547-558 (1993).
36. Mai, K.M., Assheuer, J.K., & Paxinos, G. Atlas of the human brain (2nd edition). *Elsevier: Academic Press*. (2004).
37. Yelnik, J., et al. A three-dimensional, histological and deformable atlas of the human basal ganglia. I. Atlas construction based on immunohistochemical and MRI data. *Neuroimage*. **34**, 618-638 (2007).
38. Bardin, E., et al. A three-dimensional histological atlas of the human basal ganglia. II. Atlas deformation strategy and evaluation in deep brain stimulation for Parkinson disease. *J. Neurosurg.* **110**, 208-219 (2009).
39. Maris, E., & Oostenveld, R. Non-parametric statistical testing of EEG- and MEG-data. *J. Neurosci. Methods*. **164**, 177-190 (2007).
40. Halliday, D.M., Rosenberg, J.R., Amjad, A.M., Breeze, P., Conway, B.A., & Farmer, S.F. A framework for the analysis of mixed time series/point process data-theory and application to the study of physiological tremor, single motor unit discharges and electromyograms. *Prog. Biophys. Mol. Biol.* **64**: 237-278 (1995).
41. Maris, E., Schoffelen, J.M., & Fries, P. Nonparametric statistical testing of coherence differences. *J. Neurosci. Methods*. **163**, 161-175 (2007).
42. Nolte, G., Bai, O., Wheaton, L., Mari, Z., Vorbach, S., & Hallet, M. Identifying true brain interaction from EEG data using imaginary part of coherency. *Clin. Neurophysiol.* **115**, 2292-2307 (2004).
43. Ozkurt, T. E., & Schnitzler, A. A critical note on the definition of phase-amplitude cross-frequency coupling. *J. Neurosci. Methods*. **201**, 438-443 (2011).
44. Schutter, D.J., & Knyazev, G.G. Cross-frequency coupling of brain oscillations in studying motivation and emotion. *Motiv. Emot.* **36**, (1), 46-54 10.1007/s11031-011-9237-6 (2012).
45. Palva, J.M., Palva, S., & Kaila, K. Phase synchrony among neuronal oscillations in the human cortex. *J. Neurosci.* **25**, (15), 3962-3972 (2005).
46. Oostenveld, R., Fries, P., Maris, E., & Schoffelen, J.M. FieldTrip: open source software for advanced analysis of MEG, EEG, and invasive electrophysiological data. *Comput. Intell. Neurosci.* **156869**, (2011).
47. Beste, C., Mückschel, M., Elben, S., Hartmann, C.J., McIntyre, C.C., Saft, C., Vesper, J., Schnitzler, A., Wojtecki, L. Behavioral and neurophysiological evidence for the enhancement of cognitive control under dorsal pallidal deep brain stimulation in Huntington's disease. *Brain. Struct. Funct.* **220**, 24441-8, doi: 10.1007/s00429-014-0805-x (2015).